

# Strain controlled thermomutability of single-walled carbon nanotubes

Zhiping Xu<sup>1</sup> and Markus J Buehler<sup>1,2,3,4</sup>

<sup>1</sup> Laboratory for Atomistic and Molecular Mechanics (LAMM), Department of Civil and Environmental Engineering, Massachusetts Institute of Technology, Room 1-235 A&B, 77 Massachusetts Avenue, Cambridge, MA 02139, USA

<sup>2</sup> Center for Computational Engineering, Massachusetts Institute of Technology, 77 Massachusetts Avenue, Cambridge, MA 02139, USA

<sup>3</sup> Center for Materials Science and Engineering, Massachusetts Institute of Technology, 77 Massachusetts Avenue, Cambridge, MA 02139, USA

E-mail: [mbuehler@MIT.EDU](mailto:mbuehler@MIT.EDU)

Received 13 January 2009, in final form 6 March 2009

Published 15 April 2009

Online at [stacks.iop.org/Nano/20/185701](http://stacks.iop.org/Nano/20/185701)

## Abstract

Carbon nanotubes are superior materials for thermal management and phononic device use due to their extremely high thermal conductivity and unique one-dimensional geometry. Here we report a systematic investigation of the effects of mechanical tensile, compressive and torsional strain on the thermal conductivity of single-walled carbon nanotubes using molecular dynamics simulation. In contrast to conventional predictions for solids, an unexpected dependence on the applied strain is revealed by the low-dimensional nature and tubular geometry of carbon nanotubes. Under tension, the thermal conductivity is reduced due to the softening of G-band phonon modes. Under compression—in contrast to the case for conventional theories for solids—geometric instabilities lower the thermal conductivity due to the scattering, shortening of the mean free path and interface resistance that arise from localized radial buckling. We find that when torsional strain is applied, the thermal conductivity drops as well, with significant reductions once the carbon nanotube begins to buckle. This thermomutability concept—the ability to control thermal properties by means of external cues—could be used in developing novel thermal materials whose properties can be altered *in situ*.

(Some figures in this article are in colour only in the electronic version)

## 1. Introduction

Carbon nanotubes (CNTs) and graphene, low-dimensional and single-atomic-layer materials, are outstanding electronic and thermal conductors [1], with many potential applications in thermal management and energy technology. These unique properties result not only from their graphitic lattice but also their low-dimensional overall structure. As expected from the large in-plane sound velocity in graphene sheets, experimental measurements have shown ultrahigh thermal conductivities for CNTs ( $3000 \text{ W m}^{-1} \text{ K}^{-1}$  [2]) and monolayer graphene ( $5300 \text{ W m}^{-1} \text{ K}^{-1}$  [3]), which is mainly contributed by phonons rather than electrons below or at room temperature [4]. Also, the highly stable

geometry with single atomic layer thickness of these materials provides them with great advantages in comparison with other high thermal conductivity materials. In materials such as diamond [5] and silicon carbide nanowires [6, 7] the surface phase is reconstructed and differs from bulk phase leading to an inhomogeneous phonon structure, and surface scattering of bulk phonons will significantly reduce the thermal conductivity. These features provide carbon nanotube related materials great potential with applications in thermal management [8] and phononic structures such as waveguides [9].

The low-dimensional nature of carbon nanotubes also gives rise to a set of interesting phenomena such as lattice soliton based energy transfer [10] and robust heat transport in nanotubes with severe structural deflection [9]. The graphitic lattice has excellent elasticity and high yield strength because

<sup>4</sup> Author to whom any correspondence should be addressed.

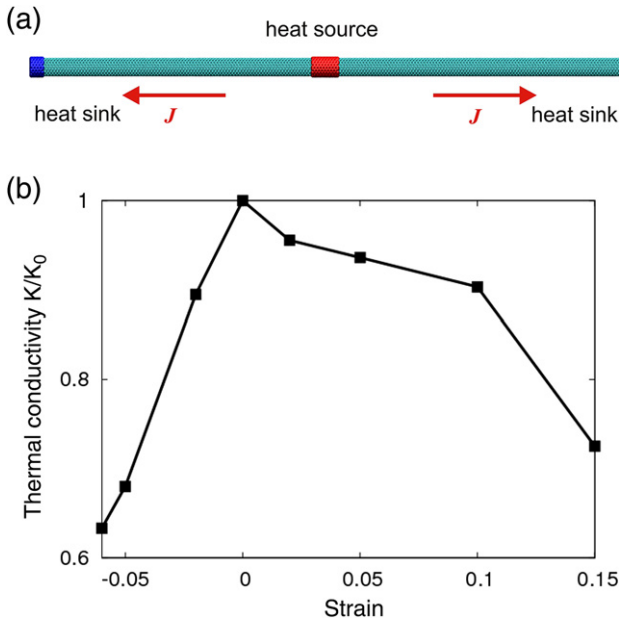


**Figure 1.** (a) The simulation setup for thermal conductivity calculation: momentum exchange is made between the hot (red, heat source) and cold (blue, heat sink) region. The hot and cold regions are nanotube segments reside in the center and edge of the simulation box with periodic boundary condition applied. Thermal conductivity  $\kappa$  is calculated from thermal flux  $J$  and temperature distribution along the transport direction. (b) Thermal conductivity of single-walled (10, 10) carbon nanotubes under strain loading from  $-0.06$  to  $0.15$ .  $\kappa_0$  is the thermal conductivity of carbon nanotube in absence of strain, which is  $301.47 \text{ W m}^{-1} \text{ K}^{-1}$ . The values for  $\kappa_0$  are lower than the experimental value ( $3000 \text{ W m}^{-1} \text{ K}^{-1}$  [2]) because the system size simulated here is shorter than the phonon mean free path ( $\sim 1 \mu\text{m}$  [4]). Results obtained here are consistent with previously reported values using the same computational method and condition [5, 24].

of the strong  $sp^2$  bonds, however, at elevated temperature or under axial compression, carbon nanotubes tend to deviate from their straight shape because of the high aspect ratio [11]. In extreme cases, the cross-section of carbon nanotubes can buckle locally from circular shapes to form ellipsoidal or dumb-bell like shapes [12]. This localized structural deformation can prohibit ballistic heat transport along the nanotube axis, as it acts as a phonon barrier [13]. These unique features of low-dimensional nanostructures pose questions on the feasibility of conventional heat conduction theory for classical solids [14].

Classical lattice thermal transport theory predicts that the thermal conductivity

$$\kappa = \sum_m C v_m l \quad (1)$$

is contributed by all the phonon modes  $m$  occupied at specific temperature ( $C$ ,  $v_m$  and  $l$  are the specific heat, group velocity and mean free path of phonon mode  $m$ ). The contribution of each mode depends on their group velocities  $v_m$  and mean free path  $l$ , while the specific heat  $C$  is considered to remain constant. Following this analysis, the modulation of thermal conductivity through mechanical deformation has

been found to generally have a monotonically decreasing function of strain, as a result from the renormalization of group velocities [15, 16]. However for one-dimensional materials such as carbon nanotubes, structural buckling occurs under compression and releases the compressive strain energy [17, 18]. Thus the conventional lattice theory for solids fails for carbon nanotubes, as will be discussed in this paper, and other models must be developed.

## 2. Theoretical and computational methods

The thermal conductivity of carbon nanotubes is calculated using molecular dynamics (MD) simulation, where the interatomic interactions are described using the AIREBO potential [19]. The thermal conductivities are calculated following Muller-Plathe's approach [20], which provides a convenient way to calculate phonon contributions to the thermal conductivity in non-equilibrium steady state. Simulations are performed using the LAMMPS MD package [21]. It is noted that the radius and chirality of carbon nanotubes can have considerable effects on their thermal conductivity. For example, the thermal conductivity is higher for carbon nanotubes with a larger radius [5], and chiral carbon nanotubes have a lower thermal conductivity than achiral ones [22]. In this paper we focus solely on strain effects on thermal properties and do not pursue studies of geometry effects. Single-walled (10, 10) carbon nanotubes of length  $L = 49.26 \text{ nm}$  are considered, with periodic boundary condition in the axial direction. The nanotube is partitioned axially into  $N_{\text{slab}} = 50$  slabs for temperature recording and control. Strain is applied to the CNT by changing the periodic simulation box size. Before calculating the thermal conductivity, 200 ps Nose-Hoover thermal bath coupling ( $T = 300 \text{ K}$ , coupling time constant  $\tau = 0.1 \text{ ps}$ , time step  $\Delta t = 0.5 \text{ fs}$ ) are conducted to reach thermal equilibration at a given applied strain. Afterward, two slabs are separated at half of the nanotube length  $L/2$ , and are chosen as heat source and sink domains (see figure 1(a) for illustration of the simulation model). A heat flux  $J$  is then injected/released subsequently in these two slabs through exchanging the momentum between the 'hottest' atom ( $mv_h^2$ ) in sink slab and the 'coldest' atom in the source slab ( $mv_c^2$ ). The momentum exchanging is performed every 20 fs. The heat flux is collected during an interval of temperature profile evaluation ( $t_{\text{transfer}}$ ), during which  $N_{\text{transfer}}$  exchanges have been performed, that is,

$$J = \frac{\sum_{N_{\text{transfer}}} \frac{1}{2} (mv_h^2 - mv_c^2)}{t_{\text{transfer}}}, \quad (2)$$

where the summation is carried out over all momentum-exchanging events, and  $t_{\text{transfer}}$  is the time period of the summation. The exchange conserves both energy and momentum of the system and converges quickly in tens of picoseconds. The whole exchanging process is performed under a  $NVE$  ensemble for 1 ns to achieve steady state. The temperature profile  $T(x)$  of the carbon nanotube is obtained after averaging over a 50 ps time interval. The thermal conductivity of carbon nanotubes is evaluated as

$$\kappa = \frac{J}{2A \partial T / \partial x}. \quad (3)$$

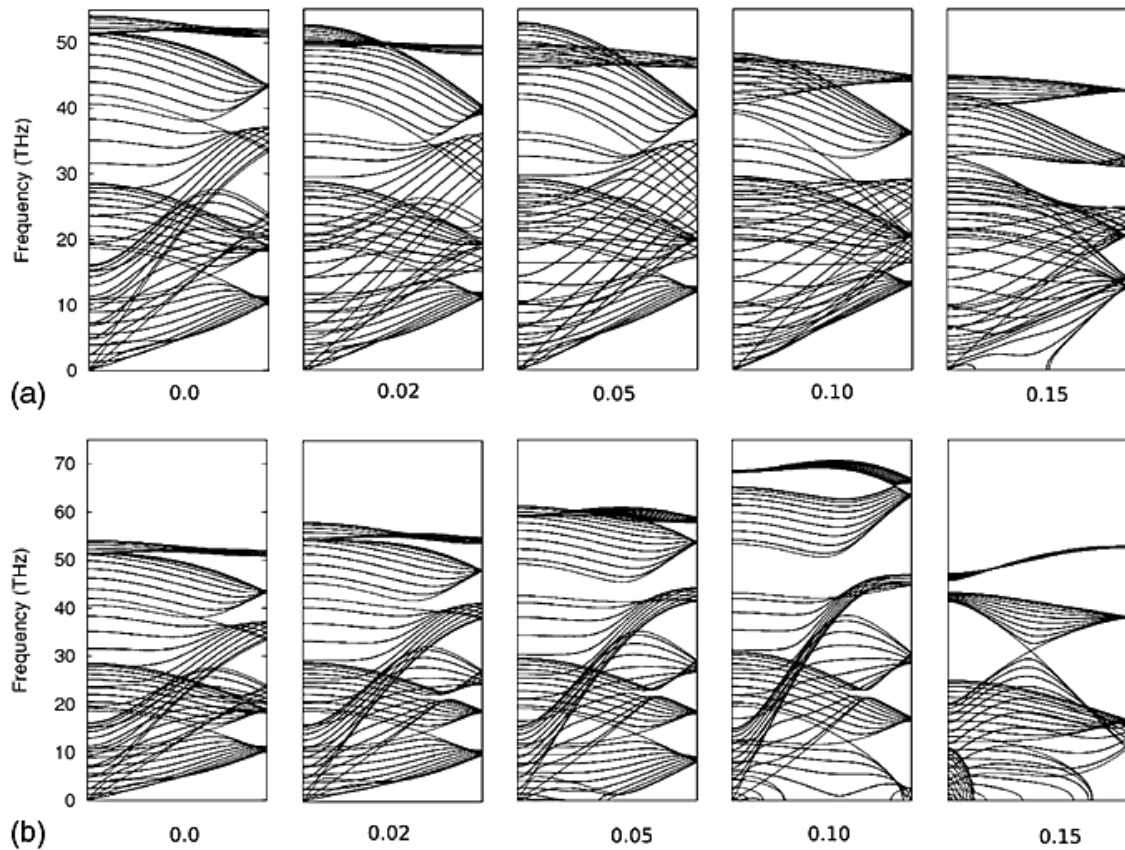


**Figure 2.** Phonon band structure under tension (a) and compression (b). The wavevectors in the figure are from  $\Gamma$  to K point. The phonon bands red-shift and the group velocity  $v_g = \partial\omega/\partial k$  decreases as the strain increases, where  $\omega$  and  $k$  is the corresponding frequency and wavevector. Also we can notice that as the positive strain increases to 0.15 or the compression strain exceeds 0.05, there are modes with negative frequencies due to local structural instabilities.

The cross-sectional area  $A$  is calculated by considering the carbon nanotubes as thin shells with thickness of a single C–C bond length. It is noted that other approaches to calculate thermal properties such as the Green–Kubo method [23] cannot be used here, as they are based on linear response theory for homogeneous system and are thus not able to describe phenomena like structural buckling of CNTs.

### 3. Results and discussion

Figure 1(b) plots the thermal conductivity of the CNT across a wide range of compressive and tensile axial strains (at 300 K), from  $-6\%$  to  $15\%$ . CNTs will break under strain values outside of this range of strains and thus will not be discussed here. It can be seen from figure 1(b) that under either positive or negative strain, the thermal conductivities of carbon nanotubes are lower than their reference value  $\kappa_0$  without strain applied, which is in contrast to the conventional prediction for solids [15, 16]. The parameter  $\kappa_0$  is the thermal conductivity of carbon nanotube in absence of strain, which is  $301.47 \text{ W m}^{-1} \text{ K}^{-1}$ . The values for  $\kappa_0$  are lower than the experimental value ( $\approx 3000 \text{ W m}^{-1} \text{ K}^{-1}$  [2]) because the system size simulated here is shorter than the phonon mean free path ( $\approx 1 \mu\text{m}$  [4]), and will increase in larger system [5]. However, the results obtained in our work are consistent

with previously reported values using the same computational method and condition [5, 24]. In the following paragraphs, we discuss the details associated with the mechanisms under tensile and compressive loading.

When the applied strain is tensile (positive), carbon–carbon bonds become elongated along the axial direction. As a consequence, the frequencies of phonon modes (especially those in the G-bands) are red-shifted (see figure 2) [25]. According to equation (1) the phonon softening will reduce group velocities and thus lower the thermal conductivity. The effects are much more pronounced when the tensile strain approaches the failure limit (at  $\approx 15\%$  for temperature of 300 K in figure 1(b)) where the thermal conductivity reduces to approximately 70% of its reference value. Phonon band structures that calculated from carbon nanotube unit cells (figure 2) show that at this large strain value close to failure, there are several phonon modes with negative frequencies, indicating that the structure is mechanically unstable.

When strain is applied in compression, the phonon modes are stiffened, as shown in our band structure calculation (figure 2). However, our MD simulations show considerable reduction of thermal conductivity under strain of  $-2\%$  and  $-5\%$ . Structural instabilities of carbon nanotubes, like Euler buckling can occur and are responsible for the observed reduction of thermal conductivity. This phenomenon contrasts

with the conventional model for three-dimensional solids [16], where compression would enhance their thermal conductivity through stiffening of phonon modes. Unlike in three-dimensional solids, single-walled carbon nanotubes are high aspect ratio cylinders composed of atomic monolayers. When the structure is compressed, the intrinsic in-plane elastic deformation can be released by transverse deflection of CNT. As observed in our simulation, when the applied strain reaches  $-2\%$ , transverse bending of the carbon nanotube is observed. The deviation of the CNT geometry from the direction of heat transfer results in unfavorable scattering of propagating waves and is responsible for the reduction of thermal conductivity. The reduction of thermal conductivity in this case is on the order of 10%, which is consistent with the experimentally observed thermal conductivity fluctuation of carbon nanotubes with bending curvature radius around 70–90 nm [9]. Thus our results provide a possible structural and mechanistic explanation for these fluctuations. In our system as shown in figure 3(b), the curved shape of the CNT in our simulation can be fitted into the parametric form

$$\mathbf{r}(t) = (A \sin(at), A \cos(at), t), \quad (4)$$

where  $\mathbf{r}$  is the spatial position of the CNT profile,  $A = 1.28$  nm,  $a = 0.013$  and  $t$  is position along the curve. Based on this expression, the radius of curvature is calculated to be  $R_c = 46.7$  nm. Nevertheless, because of the ultrahigh thermal conductivity of carbon nanotubes in comparison with conventional materials like copper, the 10% reduction observed here (and in [9]) shows that the rather high values of thermal conductivities are maintained even under bending deformation.

When the compressive strain increases to  $-5\%$ , localized buckling is observed instead of small strain bending (see figure 3(c)), and the cross-section of carbon nanotube collapses into a flattened shape (see inset in figure 3). The collapsed shape is flat with a distance of 0.35 nm between top and bottom graphene sheets. The buckle is almost immobile throughout the entire simulation. The local distortion of the cross-sections breaks the symmetry of propagating waves inside CNTs and induces a mismatch of the phonon modes between the flattened region and other segments of the CNTs that still feature cylindrical cross-sections. This interface scatters the phonon waves propagating in the carbon nanotube. As a result, the thermal conductivity of carbon nanotube was found to decrease by 32% compared to its reference value.

We proceed with a detailed analysis of the phonon spectra under different types and magnitudes of loading to elucidate the physical basis for the change of thermal properties. The phonon spectra function  $A(\omega)$  is calculated from Fourier transform of the velocity auto-correlation function  $C(\tau) = \langle \mathbf{v}(t)\mathbf{v}(t + \tau) \rangle$ .  $\langle \dots \rangle$  denotes ensemble averaging, which is substituted by averaging over velocity  $v$  at simulation time  $t$ , and over all atoms in practice. The sample velocities are taken from simulation every 1 fs and the averaging is performed over 50 ps after the system is equilibrated for 200 ps. Figure 4(a) shows the phonon spectrum of single-walled (10, 10) carbon nanotube under different strain. Under positive strain, the tension softens the G-bands remarkably in comparison with other part of the spectrum, lowers their

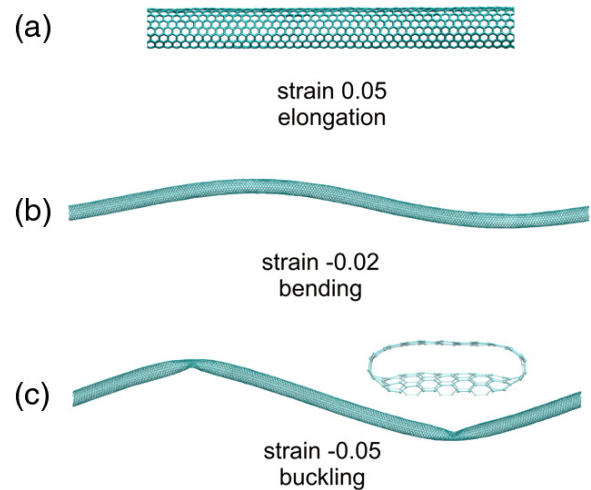


**Figure 3.** Snapshots of single-walled (10, 10) carbon nanotubes under (a) 5%, (b)  $-2\%$  and (c)  $-5\%$  strain. Positive strain (a) induces elongation of bonds along the axial direction but retains the tubular geometry. The homogeneous distortion of hexagonal lattice softens the phonon frequencies and reduces their group velocities. The structure keeps stable up to strain of 15%, beyond which the  $sp^2$  bonds start to break around their breaking limit (16%). In contrast, compression induces instabilities at rather small strain value. When strain equals to  $-2\%$ , Euler buckling occurs and the nanotube deviates from straight configuration. Transverse bending observed in the simulation has a radius of curvature of 46.7 nm. At higher strain at  $-5\%$  (c), the carbon nanotube buckles locally and collapsed into flat cross-sections (see inset). The buckles introduce phonon barriers that finally result in a 32% reduction of thermal conductivity.

group velocities and weakens the axial energy transfer. At negative strains, structural instabilities and fluctuations result in a flatter spectrum. However because the in-plane strain energy is released via buckling, the peak for G-bands does not shift. In addition, at  $-2\%$  strain where the carbon nanotube fluctuates in a spiral shape, the contribution of low-frequency mode is significant, which reflects transverse bending motion of the nanotube.

For  $-5\%$  (compressive) strain, local buckling stabilize the transverse fluctuation as observed at  $-2\%$  strain, and remove the spectrum peak at low frequencies. The positions of G-band peaks and the overall shape of the spectrum do not change too much in this case, while the thermal conductivity has been reduced by 32%. The reason for this is the increased interface resistance at the buckles. Figure 4(b) plots the temperature profile as a function of position of carbon nanotube segments. The temperature suddenly drops at the buckles (with spatial extent less than 1 nm), and results in an interface (or Kapitza) conductivity of approximately  $\kappa_{\text{interface}} = 50$  GW  $m^{-2}$   $K^{-1}$ . The interface thermal conductivity is defined as  $\kappa_{\text{interface}} = J/2A\Delta T$ , where  $J$  is the thermal flux,  $A$  is cross-sectional area and  $\Delta T$  is the temperature drop at the interface. Considering the thermal conductivity of carbon nanotubes without strain  $\kappa_0 = 301.47$  W  $m^{-1}$   $K^{-1}$ , this local buckling is equivalent to a segment of carbon nanotubes with a length of  $l = \kappa_0/\kappa_{\text{interface}} = 6$  nm. Larger compressive strain of  $-6\%$  reveals similar phenomenon with a lower interface conductivity of 33 GW  $m^{-2}$   $K^{-1}$ . Further compression at 300 K will break

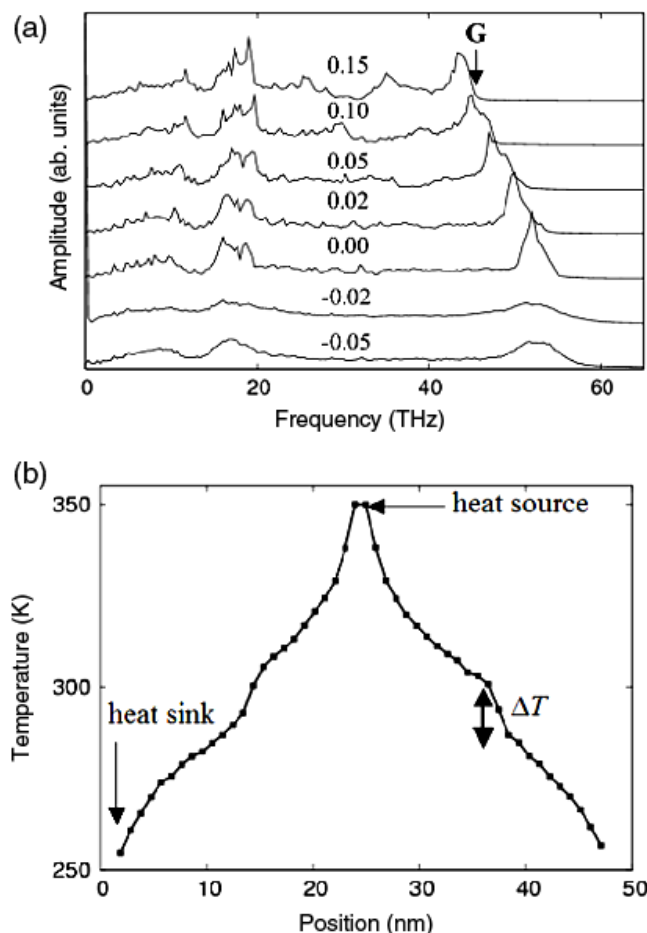


**Figure 4.** (a) Phonon spectrum of single-walled (10, 10) carbon nanotube under strain from  $-5\%$  to  $15\%$ . At positive strain, the tension softens the G-band significantly and weakens the axial energy transfer. At negative strain, structural instability results in a flatter spectrum. At compression of  $-2\%$  strain, remarkable contribution from low-frequency bending mode arises. (b) Temperature profile along the axial position, when the nanotube buckles locally due to the compression. The temperature suddenly drops  $\sim 13$  K at the buckles (approximately 1 nm), results in an interface (Kapitza's) conductivity  $\sim 50$  GW  $m^{-2}$   $K^{-1}$ . This interface resistance is equivalent to a segment of carbon nanotubes with length of 6 nm. The Kapitza's thermal interface conductivity is defined as  $\kappa_{\text{interface}} = J/(A\Delta T)$ , where  $J$  is the heat flux across the interface and  $A$  is the area of cross-section and  $\Delta T$  is the temperature jump.

the carbon nanotube and thus not investigated here for thermal conductivity.

Torsional strain provides another approach to control the thermal properties of carbon nanotubes. To investigate its effect on thermal conductivity, twisting strain up to  $0.039$   $\text{\AA}^{-1}$  is applied within the breaking limit. To implement torsional loading in the system with periodic boundary conditions, we take advantage of the  $D_{10}$  symmetry of (10, 10) carbon nanotube. A torsional strain of  $n2\pi/L$  can be applied, where  $n$  is an integer and  $L$  is the length of simulation box along tube axis. As shown in figure 5, at twist strain less than  $0.065$ , the carbon nanotube preserves its cylindrical shape and the thermal conductivity changes only by around  $1\%$ . However, when the strain increases up to  $0.013$ , the carbon nanotubes starts to

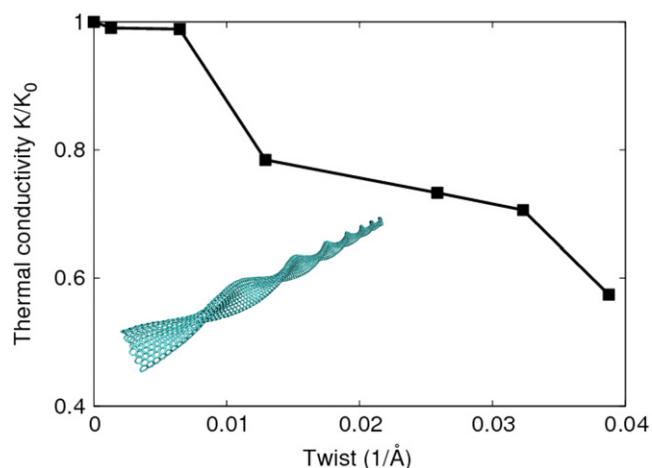


**Figure 5.** Thermal conductivity of single-walled (10, 10) carbon nanotubes under strain loading from 0 to  $0.039$   $\text{\AA}^{-1}$  at 300 K. The thermal conductivity drops significantly at strain  $0.013$  because the cross-sections of carbon nanotubes begin to buckle. Inset: snapshot of (10, 10) carbon nanotube at twist strain of  $0.026$ , when the cross-sections collapse.

buckle (see inset in figure 5) in the cross-section. The buckling is uniform along the axis of carbon nanotube except for the rotation due to twist. The radial geometrical change results in a significant drop of the thermal conductivity on the order of  $20\%$ .

#### 4. Discussion and conclusion

Our study unveils that mechanical strain has a distinct effect on the thermal transfer properties of CNTs, where the mechanisms change under tensile, compressive and torsion loading and also depend on the magnitude of the strain applied. In tensile deformation, the thermal conductivity is reduced to  $30\%$  at the point of mechanical failure; in compression, the reduction reaches  $10\%$  in a regime of homogeneous bending and reaches  $32\%$  when localized buckling occurs. In torsion, the radial buckling is also responsible for the  $20\%$  reduction of the thermal conductivity, with a similar underlying mechanism due to local buckling. The three distinct mechanisms (phonon softening, delocalized bending and localized buckling) under uniaxial and torsional strain are phenomena closely linked to the particular one-dimensional and tubular structure of carbon nanotubes. Similar phenomena may thus also hold for other one-dimensional materials such as solid nanowires and graphene nanoribbons.

In addition to the fundamental insight into the physical mechanisms, the results reported in this paper feature potential for several nanotechnology applications. For example, arrays or circuits of carbon nanotubes could be fabricated whose thermal transfer performance can be tuned reversibly through external mechanical cues, in a continuous way (e.g. through application of positive tensile strain), or as a 'discrete' switch (e.g. by taking advantage of buckling induced by compressive loading). This thermomutability concept, the ability to control thermal properties by external cues, could

be used in adaptive thermal control and management. In such applications, thermomutable properties could be exploited to develop multifunctional metamaterials that feature hierarchical structures at multiple levels to provide a superior material performance, self-organization and controllability. The strain dependence of thermal conductivity might be utilized also in sensor applications, where local strains could be inferred from measuring temperature distributions. Furthermore, the robustness of high thermal conductivity of CNTs under large deflection reveals their capability to serve as constituents of stretchable and foldable thermal bulk materials. Our study provides insight into which levels of local strains can be tolerated by carbon nanotubes while still providing sufficient thermal properties.

## Acknowledgments

This work was supported by DARPA and the MIT Energy Initiative (MITEI). This work was supported in part by the MRSEC Program of the National Science Foundation under award number DMR-0819762.

## References

- [1] Saito R, Dresselhaus G and Dresselhaus M S 1998 *Physical Properties of Carbon Nanotubes* (London: Imperial College Press)
- [2] Kim P, Shi L, Majumdar A and McEuen P L 2001 Thermal transport measurements of individual multiwalled nanotubes *Phys. Rev. Lett.* **87** 215502
- [3] Balandin A A, Ghosh S, Bao W, Calizo I, Teweldebrhan D, Miao F and Lau C N 2008 Superior thermal conductivity of single-layer graphene *Nano Lett.* **8** 902–7
- [4] Hone J, Whitney M, Piskoti C and Zettl A 1999 Thermal conductivity of single-walled carbon nanotubes *Phys. Rev. B* **59** R2514
- [5] Padgett C W, Shenderova O and Brenner D W 2006 Thermal conductivity of diamond nanorods: molecular simulation and scaling relations *Nano Lett.* **6** 1827–31
- [6] Mingo N, Yang L, Li D and Majumdar A 2003 Predicting the thermal conductivity of Si and Ge nanowires *Nano Lett.* **3** 1713–6
- [7] Ponomareva I, Srivastava D and Menon M 2007 Thermal conductivity in thin silicon nanowires: phonon confinement effect *Nano Lett.* **7** 1155–9
- [8] Kordas K, Toth G, Moilanen P, Kumpumaki M, Vahakangas J, Uusimaki A, Vajtai R and Ajayan P M 2007 Chip cooling with integrated carbon nanotube microfin architectures *Appl. Phys. Lett.* **90** 123105
- [9] Chang C W, Okawa D, Garcia H, Majumdar A and Zettl A 2007 Nanotube phonon waveguide *Phys. Rev. Lett.* **99** 045901
- [10] Chang C W, Okawa D, Majumdar A and Zettl A 2006 Solid-state thermal rectifier *Science* **314** 1121–4
- [11] Deng F, Zheng Q-S, Wang L and Nan C 2007 Effects of anisotropy, aspect ratio, and nonstraightness of carbon nanotubes on thermal conductivity of carbon nanotube composites *Appl. Phys. Lett.* **90** 021914
- [12] Dresselhaus M S, Dresselhaus G and Avouris P 2000 *Carbon Nanotubes: Synthesis, Structure, Properties and Applications* (Berlin: Springer)
- [13] Cahill D G, Ford W K, Goodson K E, Mahan G D, Majumdar A, Maris H J, Merlin R and Phillpot S R 2003 Nanoscale thermal transport *J. Appl. Phys.* **93** 793–818
- [14] Chen G 2005 *Nanoscale Energy Transport and Conversion* (Oxford: Oxford University Press)
- [15] Picu R C, Borca-Tasciuc T and Pavel M C 2003 Strain and size effects on heat transport in nanostructures *J. Appl. Phys.* **93** 3535–9
- [16] Somnath B and Vijay B S 2006 Effect of strain on the thermal conductivity of solids *J. Chem. Phys.* **125** 164513
- [17] Buehler M J, Kong Y and Gao H J 2004 Deformation mechanisms of very long single-wall carbon nanotubes subject to compressive loading *J. Eng. Mater. Technol.* **126** 5
- [18] Buehler M J 2006 Mesoscale modeling of mechanics of carbon nanotubes: self-assembly, self-folding and fracture *J. Mater. Res.* **21** 15
- [19] Brenner D W, Shenderova O A, Harrison J A, Stuart S J, Ni B and Sinnott S B 2002 A second-generation reactive empirical bond order (REBO) potential energy expression for hydrocarbons *J. Phys.: Condens. Matter* **14** 783–802
- [20] Florian M-P 1997 A simple nonequilibrium molecular dynamics method for calculating the thermal conductivity *J. Chem. Phys.* **106** 6082–5
- [21] Plimpton S 1995 Fast parallel algorithms for short-range molecular dynamics *J. Comput. Phys.* **117** 1–19
- [22] Zhang W, Zhu Z, Wang F, Wang T, Sun L and Wang Z 2004 Chirality dependence of the thermal conductivity of carbon nanotubes *Nanotechnology* **15** 936
- [23] Che J, Cagin T and Goddard W A III 2000 Thermal conductivity of carbon nanotubes *Nanotechnology* **11** 65
- [24] Pan R, Xu Z, Zhu Z and Wang Z 2007 Thermal conductivity of functionalized single-wall carbon nanotubes *Nanotechnology* **18** 285704
- [25] Cronin S B, Swan A K, Unlu M S, Goldberg B B, Dresselhaus M S and Tinkham M 2004 Measuring the uniaxial strain of individual single-wall carbon nanotubes: resonance Raman spectra of atomic-force-microscope modified single-wall nanotubes *Phys. Rev. Lett.* **93** 167401